ASSESSING FUTURE GREENHOUSE GAS CONCENTRATIONS IN MADRID, SPAIN: A DYNAMICAL DOWNSCALING APPROACH USING WRF-VPRM

Roberto San Jose, Juan L. Perez-Camanyo and Miguel Jimenez-Gañan

Environmental Software and Modelling Group, Computer Science School, Technical University of Madrid (UPM), Madrid, Spain.

E-mail address of the corresponding author: roberto@fi.upm.es

Preprint: Air Quality, Atmosphere & Health (2025) 18:3813–382 .https://doi.org/10.1007/s11869-025-01798-1cities

ACKNOWLEDGEMENTS

DISTENDER has received funding from the European Union's Horizon EU research and innovation programme under grant agreement No 101056836.

The UPM co-authors acknowledge the computer resources and technical assistance provided by the Centro de Supercomputación y Visualización de Madrid (CeSViMa). The UPM co-authors thankfully acknowledge the computer resources, technical expertise and assistance provided by the Red Española de Supercomputación (RES)

ABSTRACT

This study employs a comprehensive modeling approach that combines the Weather Research Forecast (WRF) model with the Vegetation Photosynthesis and Respiration Model (VPRM) to gain insights into the intricate dynamics of GHGs flux and concentration. The primary objective is to conduct high-resolution simulations of GHGs transport, dispersion, and concentrations spanning from 2015 to 2050 under future climate scenario over Madrid (Spain) region. The global climate scenarios datasets are provided by the 6th Coupled Model Intercomparison Project (CMIP6). Dynamical downscaling is done by the WRF model to increase the spatial resolution of the climate data. The results of the atmospheric simulations illuminate the impact (future – present) of emission source distribution and climate data on GHG concentrations. Additionally, the incorporation of the vegetation photosynthesis and respiration model provides valuable perspectives on the role of terrestrial ecosystems in the global carbon cycle and their influence on atmospheric CO2 concentrations.

Keywords: Climate Change, CO2, VPRM

1. INTRODUCTION

Carbon dioxide (CO_2) is a long-lived greenhouse gas (GHG) in the atmosphere that plays an important role in the Earth's climate system. Concentrations of CO2 in the atmosphere come from both anthropogenic and natural sources, as well as anthropogenic (fuel combustion) and natural sources (biogenic fluxes from ecosystems). In recent decades, atmospheric concentrations of CO_2 have increased significantly, largely due to human activity as anthropogenic CO_2 emissions exceed the CO2 sequestration capacity of terrestrial ecosystems and oceans. Quantifying the exchange of CO_2 between the atmosphere and terrestrial ecosystems (biogenic fluxes) is essential for understanding the carbon balance and accurately identifying sources and sinks. Urban areas, in particular, are the largest contributors to global CO_2 emissions, accounting for more than 70% of total anthropogenic emissions (IPCC,2014). In response, many cities around the world have committed to achieving net GHG emissions by 2050. However, achieving this target requires robust methodologies for the quantification of anthropogenic (Davis et al., 2017) and biogenic CO2 emissions with high spatial resolution. From this information, effective mitigation actions can be designed. Anthropogenic emission inventories have been developed to estimate CO_2 emissions in all sectors, including industry, transport, residential and commercial activities (Sówka and Bezyk, 2018). These inventories are continuously refined to improve temporal and spatial resolution. In parallel, natural fluxes - especially those driven by interactions between the biosphere and the atmosphere - introduce additional complexity into CO_2 concentration dynamics. These biogenic fluxes are highly sensitive to meteorological conditions, such as temperature, solar radiation and land cover type, and can significantly influence CO2 balances. Despite advances in observation networks and modelling capabilities, CO_2 fluxes at regional/local scales remain insufficiently characterised due to their large spatial and temporal variability, especially in heterogeneous environments with complex urban and vegetation mosaics. To address this challenge, mesoscale atmospheric models such as the Weather Research and Prediction coupled with Chemistry and the Plant Respiration and Photosynthesis Model (WRF/Chem-VPRM) have been developed. These models allow simultaneous simulation of meteorological fields, CO_2 transport and biospheric exchange with high spatial and temporal resolution.

While global climate models (GCMs), such as those used in the Sixth Assessment Report of the Intergovernmental Panel on Climate Change (IPCC AR6), provide valuable information on global trends under various Shared Socio-Economic Pathways (SSPs), their coarse resolution limits their usefulness for analysing local and regional climate impacts. GCMs often do not capture fine-scale phenomena, such as local wind patterns, land-use heterogeneity or topographic effects, which are crucial for accurate CO_2 modelling. Downscaling techniques, in particular dynamic downscaling with regional climate models (RCMs), are therefore essential for translating global climate projections into practical information at regional scales. Dynamic downscaling allows RCMs to incorporate regional physiographic features such as elevation, vegetation and urban structure, improving their ability to simulate climate variables and their corresponding effects on biogenic emissions and CO_2 concentrations (Dong et al., 2021). In this context, the present study investigates the high-resolution impact of future climate scenarios on CO_2 fluxes in the Iberian Peninsula, Community of Madrid and Municipality of Madrid, using a nested modelling approach with the WRF/Chem-VPRM model driven by the climate scenarios that are dynamically rescaled, offering a multi-scale perspective of carbon dynamics. The analysis covers the period from 2015 to 2050 and focuses on isolating the influence of future climate conditions on biogenic CO_2 emissions and total atmospheric CO_2 concentrations. To ensure consistency, anthropogenic emissions and land use are held constant at 2018 levels, allowing the climate signal to emerge as the dominant driver of change. This methodology offers a unique opportunity to assess how future climate changes - under different SSPs - may modulate biospheric CO_2 exchange and impact CO2 mitigation strategies.

Although CMIP6 (Eyring et al., 2016) GCMs represent a major step forward in climate modelling, offering better spatial resolution and more sophisticated physical parameterisations compared to their CMIP5 predecessors, they still exhibit significant biases in regional climate simulation, especially in complex terrain or extreme conditions (Zhu and Yang, 2020; Hu and Zhou, 2021; Cui et al., 2021). These limitations underline the importance of regional downscaling in producing reliable climate information for urban- and regional-scale carbon modelling. In this study, the use of rescaled CMIP6 climate scenarios in combination with high-resolution CO_2 modelling addresses a critical knowledge gap: how future climate change might influence biospheric CO_2 emissions in an urban context. By assessing climate-driven changes in net carbon exchange in the Madrid region, this work contributes to a better understanding of the interactions between regional climate dynamics and the carbon cycle, an essential step towards designing effective mitigation strategies for climate-resilient cities.

In this study, four climate scenarios from CMIP6 were considered to assess the potential impacts of future climate conditions on biogenic CO_2 emissions and concentrations. These scenarios correspond to the Tier 1 Shared Socioeconomic Pathways (SSPs), which combine different trajectories of socioeconomic development (Meinshausen et al., 2020) with associated greenhouse gas emissions and radiative forcing levels projected for the year 2100. The selected scenarios—SSP1-2.6, SSP2-4.5, SSP3-7.0, and SSP5-8.5—span a wide range of plausible future climate outcomes and represent different levels of mitigation and adaptation challenges (O'Neill et al., 2016; Riahi et al., 2017).

SSP1-2.6 represents a sustainability-oriented pathway, often referred to as the "green road." It assumes low challenges to both mitigation and adaptation, with strong international cooperation, rapid technological advancement, and a shift towards environmentally friendly energy systems. The scenario targets a low radiative forcing of 2.6 W/m² by 2100, roughly consistent with the Paris Agreement goal of limiting global warming to below 2°C. It is analogous to the RCP2.6 pathway used in CMIP5 and reflects ambitious climate protection efforts.

SSP2-4.5, known as the "middle-of-the-road" scenario, assumes intermediate challenges to mitigation and adaptation. It envisions a world that follows historical patterns, with moderate progress in sustainability and climate policy. This pathway results in a radiative forcing of 4.5 W/m² by the end of the century and serves as a baseline scenario for many climate impact assessments. It is considered a direct update to RCP4.5 from the previous CMIP5 framework.

SSP3-7.0 portrays a fragmented world characterized by regional rivalry and slow economic development. Under this pathway, national priorities dominate over global cooperation, and mitigation efforts are limited. As a result, greenhouse gas emissions rise substantially, leading to a radiative forcing of 7.0 W/m² by 2100. This scenario reflects a high-challenge context for both mitigation and adaptation and is indicative of policy failure in achieving international climate targets.

SSP5-8.5 represents a fossil-fueled development pathway, often described as the "highway" scenario. It envisions rapid economic growth powered by continued reliance on carbon-intensive energy sources such as coal, oil, and natural gas. While adaptation capacity may increase due to technological advancement and economic strength, mitigation efforts remain minimal. This scenario leads to a radiative forcing of 8.5 W/m² by 2100, making it the most extreme of the four in terms of climate change impacts and comparable to RCP8.5 in CMIP5. It serves as an upper-bound scenario for assessing worst-case outcomes (Hausfather & Peters, 2020).

Previous studies have demonstrated the value of WRF-VPRM modelling system in capturing biogenic CO_2 dynamics (Mahadevan et al., 2008; Ahmadov et al., 2009). This model is based on satellite-derived vegetation indices and meteorological data obtained by WRF to simulate two key components of biogenic carbon flux: gross ecosystem exchange (GEE) and ecosystem respiration (ER). Numerous applications of WRF/Chem-VPRM in Europe, Asia and North America have demonstrated their ability to capture mesoscale transport patterns and vegetation-driven variability (Ballav et al., 2012; Pillai et al., 2016; Park et al., 2018). Urban ecosystems, in particular, exhibit strong seasonal and diurnal variability in CO_2 uptake, influenced by vegetation phenology (Hutyra et al., 2014), microclimate and anthropogenic activity (; Hardiman et al., 2017; Miller et al., 2020; Bezyk et al., 2021). Consequently, future changes in temperature, radiation and moisture availability may significantly alter the balance between biogenic uptake and release, especially during extreme events such as heat waves or droughts.

2. METHODOLOGY

2.1 Experiment

To assess the impact of future climate conditions on biogenic emissions and atmospheric CO_2 dynamics, a comprehensive numerical experiment was carried out using the WRF/Chem-VPRM modelling system, which will be described in more detail in the next section. The simulations cover a nested domain configuration centred (40.478°N, 3.704°W) over Madrid (Spain) covering the Iberian Peninsula, the Community of Madrid and the Madrid metropolitan area. The model employs a two-way interactive nesting approach across three spatial domains: Domain 1 (D1): 27 km horizontal resolution. Domain 2 (D2): 9 km

horizontal resolution Domain 3 (D3): 3 km horizontal resolution Each domain is structured as a 30 × 30 grid with 33 vertical atmospheric layers extending from the surface to 10 hPa.

The simulation period spans 35 years, from 2015 to 2050, with a start-up period of one day used to initialise the atmospheric state each year. The simulations were run continuously for one year, generating hourly results for each of the three spatial domains and the four CMIP6 Tier 1 climate scenarios (SSP1-2.6, SSP2-4.5, SSP3-7.0 and SSP5-8.5). The computational workload was distributed over 120 parallel jobs, each running on 9 cores, accumulating a total of approximately 50,000 CPU hours and producing over 10 TB of output data.

The climate forcing for the WRF/Chem-VPRM simulations was obtained from the six-hourly outputs available in the CMIP6 repositories of the Max Planck Institute Earth System Model (MPI-ESM1.2-HR), an Earth system model that has an atmospheric component based on ECHAM6.3, with a horizontal resolution of T127 (approximately 0.93° × 0.93° or ~103 km) and 95 vertical levels extending down to 0.01 hPa. The ocean model is MPIOM1.63, with a resolution of TP04 (0.4° × 0.4° or ~44 km) and 40 vertical levels. This particular GCM was selected because it is explicitly tuned to a 3 K equilibrium climate sensitivity, and a well-balanced radiation budget (Müller et al., 2018). These features make MPI-ESM1.2-HR particularly suitable for regional downscaling and impact assessment applications. Historical climate simulations cover the period 1980-2014, while future projections cover 2015-2100. For this study, the period from 2015 to 2050 was extracted and dynamically rescaled, and initial and lateral boundary conditions for meteorological variables were updated every six hours using the output of MPI-ESM1.2-HR.

2.2 Modelling system

The simulation chain begins with the conversion of CMIP6 six hours GCM outputs (2015-2050) into WRF-compatible intermediate files using the `cmip6-to-wrfinterm` Python tool (https://github.com/lzhenn/cmip6-to-wrfinterm), which will be read by the WRF Preprocessing System (WPS) with the 2018 (reference year) land use and topographic data. Next, WRF/Chem-VPRM model is executed using the initial and boundary conditions from WPS and 2018 anthropogenic emissions. During the simulation (on-line) VPRM calculates biogenic CO_2 fluxes at each time step using vegetation indices, simulated temperature, and radiation. These fluxes are then transported by the chemistry module within WRF/Chem. WRF/Chem is a fully compressible, non-hydrostatic meteorological (WRF) and chemical transport (Chem) model developed by NCAR (Grell et al., 2005). It integrates atmospheric dynamics and chemical processes in an online framework, ensuring consistency in physics, transport, and emissions across the meteorological and chemical components (Powers et al., 2017). In this study, WRF-Chem version 4.1.5 is used, with the following physical parameterization: Microphysics: Morrison double-moment scheme (Morrison et al., 2009). Radiation: Rapid Radiative Transfer Model for GCMs (RRTMG) for both shortwave and longwave (Iacono et al. 2008). Planetary Boundary Layer (PBL): Yonsei University (YSU) scheme (Hong et al. 2006). Surface Layer: Monin-Obukhov scheme (Monin and Obukhov 1954). Land Surface: Noah LSM (Tewari et al., 2004). Cumulus Parameterization: Grell 3D Ensemble (G3) (Grell and Dévényi 2002). CO_2 Chemistry: Passive tracer mode (no chemical reactions).

Anthropogenic CO_2 emissions are based on the CAMS-GLOB-ANT emission inventory, downscaled using the EMIMO emission model developed at UPM (San Jose et al, 2015). This inventory provides hourly gridded emissions at 0.1° × 0.1° resolution for the year 2018. The biogenic emissions are calculated by VPRM module. The VPRM (Mahadevan et al., 2008; Ahmadov et al., 2007) is a model that estimates Net Ecosystem Exchange (NEE) of CO_2 as the difference between Gross primary production (GPP, uptake) and ecosystem respiration (R, release). GPP and R are calculated by the equations 1 and 2.

$$GPP = \lambda \times Tscale \times Pscale \times Wscale \times FAPAR_{PAV} \times [PAR / (1 + PAR / PAR_0)] \quad (1)$$

$$R = \alpha \times T_{air} + \beta \quad (2)$$

Where:

λ, α, β, PAR_0 are empirical parameters dependent on the eight land cover types, optimized by Europe.

T_{air} is 2 m air temperature from WRF

PAR is the Photosynthetically Active Radiation, derived as 0.5 × downward shortwave radiation (SW) from WRF.

Tscale, Pscale and Wscale are three dimensionless scaling factors related with the temperature sensitivity of photosynthesis, effects of leaf age on canopy photosynthesis and water stress effect respectivily. They are dependents from EVI (Enhanced Vegetation Index**)** and LSWI indices (Land Surface Water Index).

These indices can be derivated from the reflectance data from the MODIS-Terra MOD09A1 v6 product, with 8-day temporal resolution and 500 m spatial resolution. The applied equations are (3) for EVI and (4) for LSWI:

$$EVI = 2.5 \times (\rho NIR - \rho RED) / (\rho NIR + 6 \times \rho RED - 7.5 \times \rho BLUE + 1) \quad (3)$$

$$LSWI = (\rho NIR - \rho SWIR) / (\rho NIR + \rho SWIR) \quad (4)$$

Where ρ values represent surface reflectance in the blue, red, near-infrared (NIR), and shortwave infrared (SWIR) bands.

3. RESULTS

Before presenting the results of the CO2-related simulations, an evaluation of the modelling system has been carried out using the temperature variable, due to its importance and data availability.

3.1 Evaluation

To evaluate the performance of the WRF/Chem-VPRM model in simulating near-surface air temperature (2 meters high) , we used hourly observed temperature data from three meteorological stations located within Domain 3 (3 km resolution). The stations are identified by: Barajas, Cuatro Vientos and Getafe which are spatially distributed across the domain. Hourly data were available from 2015 to 2024, a total of 72,959 valid hourly observations per station. The hourly values of the 3 stations (station 0) were also averaged to be compared with the mean values of the three cells where the stations are located. For each model simulation corresponding to the four CMIP6-based climate scenarios (SSP1-2.6, SSP2-4.5, SSP3-7.0, and SSP5-8.5), model results were compared with observed data. The comparison included two standard performance metrics, such as the coefficient of determination (R^2), and the normalised mean bias (NMB). The results are showed in Table 1, the table below summarizes the NMB and R^2 values for each scenario and station

Table 1: Performance metrics

Simulation	**Station**	**NMB**	**R^2**
ssp126	0	0,44	0,84
ssp245	0	0,2	0,82
ssp370	0	0,41	0,83
ssp585	0	0,36	0,84
ssp126	1	0,33	0,84
ssp245	1	0,43	0,83
ssp370	1	-0,2	0,83
ssp585	1	0,17	0,85
ssp126	2	0,24	0,81
ssp245	2	0,1	0,81
ssp370	2	-0,2	0,81
ssp585	2	0,04	0,82
ssp126	3	0,32	0,84
ssp245	3	0,16	0,83
ssp370	3	-0,4	0,84
ssp585	3	0,17	0,85

Overall, the WRF/Chem-VPRM model shows a high ability to reproduce the temporal evolution of hourly temperature, with R^2 values above 0.80 for all scenarios and stations. These high correlation coefficients indicate that the model is able to accurately capture the variability and trends in observed temperature over the eight-year period. In particular, the best agreement was found for the SSP5-8.5 scenario, which achieved the highest R^2 values (up to 0.85) and the lowest bias values, suggesting that it is the most representative of recent climate conditions in the region. We can therefore consider SSP5-8.5 as the reference scenario or Business As Usual (BAU).

However, despite the high correlation, a consistent positive bias is observed in most simulations, where modelled temperatures generally underestimate actual values. This bias is present in all scenarios except SSP3-7.0, where a negative bias is recorded. It is important to note that the grid-cell-based nature of the model introduces an inherent spatial averaging, which can dampen the magnitude of extreme events compared to point-based observations. Increasing the spatial resolution above 3 km could improve the model's ability to capture these more point-based variations, however, given the 35-year simulation horizon and associated computational burden this refinement is beyond the scope of the present work.

3.2 Spatial distribution

The following images include a set of maps showing the results derived from computational simulations. These images clarify the spatial dispersion patterns of various simulated parameters across various spatial scales. Each map provides insight into the spatial distribution of the simulated variables, outlining their respective patterns and variations across the study area. Figure 1 shows the spatial distribution of the CO_2 emission budget, comprising the cumulative sum of biogenic (which may be negative in some areas in case of absorption dominance) and anthropogenic emissions, in the context of the SSP5-8.5 climate scenario. The figure corresponds to simulations performed at spatial resolutions of 27 km (left) and 3 km (right), respectively. The data shown are mean values derived from hourly data averaged over the entire 35-year simulation period.

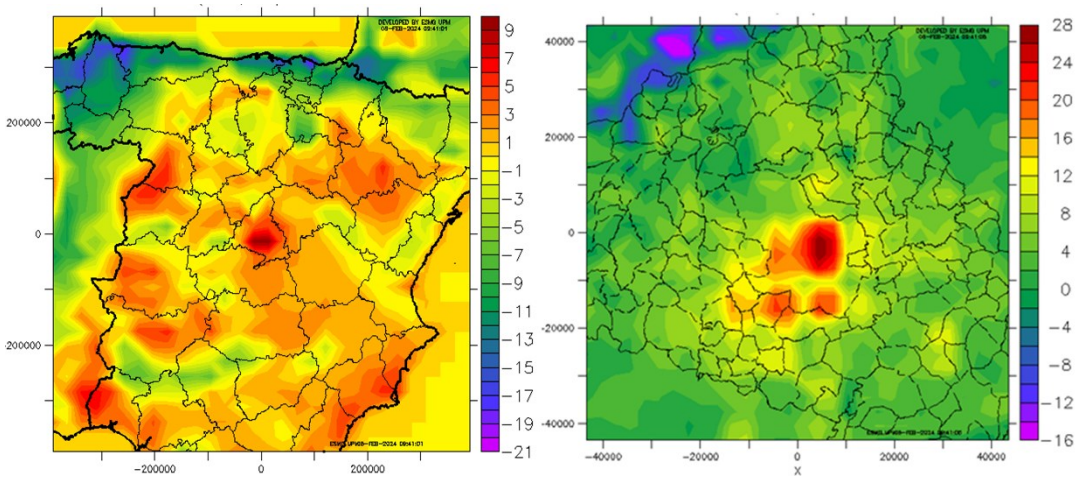

Figure 1. Spatial distributions of simulated CO_2 emissions (kmol km-2 hr-1) budget (biogenic + anthropogenic contributions). Mean of 35 years 2015-2050 from WRF/Chem-VPRM simulation (27 km) for SSP585 scenario.

In Figure 1, the Iberian Peninsula (left) shows a combination of areas with a negative net balance, indicative of CO_2 absorption, together with areas characterised by predominant CO_2 emissions, as clearly seen in the central area of the image where the city of Madrid is located, where anthropogenic emissions are very high. In addition, the northern regions of Spain and Portugal present important CO_2 sinks as they are areas of dense vegetation. Right part of Figure 1 provides a more detailed examination of the Madrid region, revealing a predominance of positive net balances, particularly important in the urban area of Madrid. In contrast, only a few isolated sites serve as CO_2 sinks, albeit with lower magnitudes than in the north of the Peninsula. These sinks are located in the mountainous area of Madrid, where the density of vegetation is higher.

Figure 2 shows the differences in expected net biogenic emissions (NEE) between the SSP3-7.0 and SSP5-8.5 climate scenarios. It shows that in the SSP3-7.0 scenario there would be an increase in biogenic CO_2

emissions in most areas of the Iberian Peninsula. This increase is due to an increase in vegetation respiration, which is favoured by the higher temperatures predicted in the SSP3-7.0 scenario compared to SSP5-8.5.

Figure 3 provides a visual representation of the spatial distribution of CO_2 concentrations within the 3 km spatial resolution domain under the SSP5-8.5 scenario. Concentrations of Figure 3 are the result of a combination of anthropogenic and biogenic emissions, boundary conditions, and CO_2 transport and diffusion under the simulated meteorological conditions. The figure clearly illustrates the dominance of anthropogenic emissions from Madrid within the region. The emitted CO_2 shifts significantly to the southwest due to the prevailing winds in the area. In contrast, the mountainous regions have the lowest CO_2 concentrations. This phenomenon can be attributed to the presence of sinks in this area, minimal anthropogenic emissions and prevailing winds that do not transport CO_2 from the city to these locations.

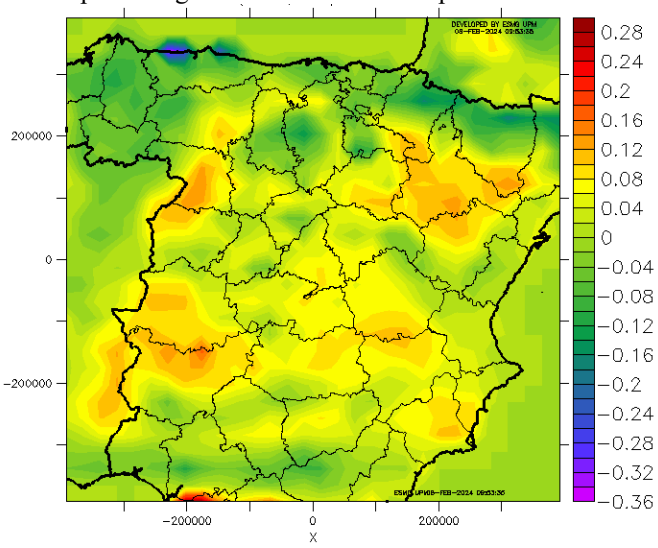

Figure 2. Spatial distributions of differences between scenarios SSP370-SSP585 for the NEE (Net Ecosystem Exchange) (kmol km-2 hr-1). Mean of 35 years 2015-2050 from WRF/Chem-VPRM simulation (27 km).

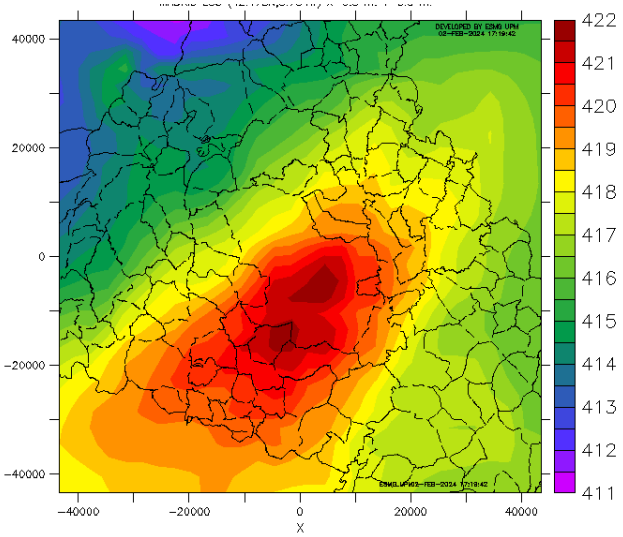

Figure 3. Spatial distributions of simulated CO_2 concentrations (ppm). Mean of 35 years 2015-2050 from WRF/Chem-VPRM simulation (3 km) for SSP585 scenario.

The figure 4 shows the annual evolution of Net Ecosystem Exchange (NEE) of CO_2, spatially averaged over the model domain, for the period 2015–2049 under four CMIP6 scenarios (SSP1-2.6, SSP2-4.5, SSP3-7.0, SSP5-8.5). Negative values indicate net CO_2 uptake by vegetation, while positive values represent net emissions to the atmosphere

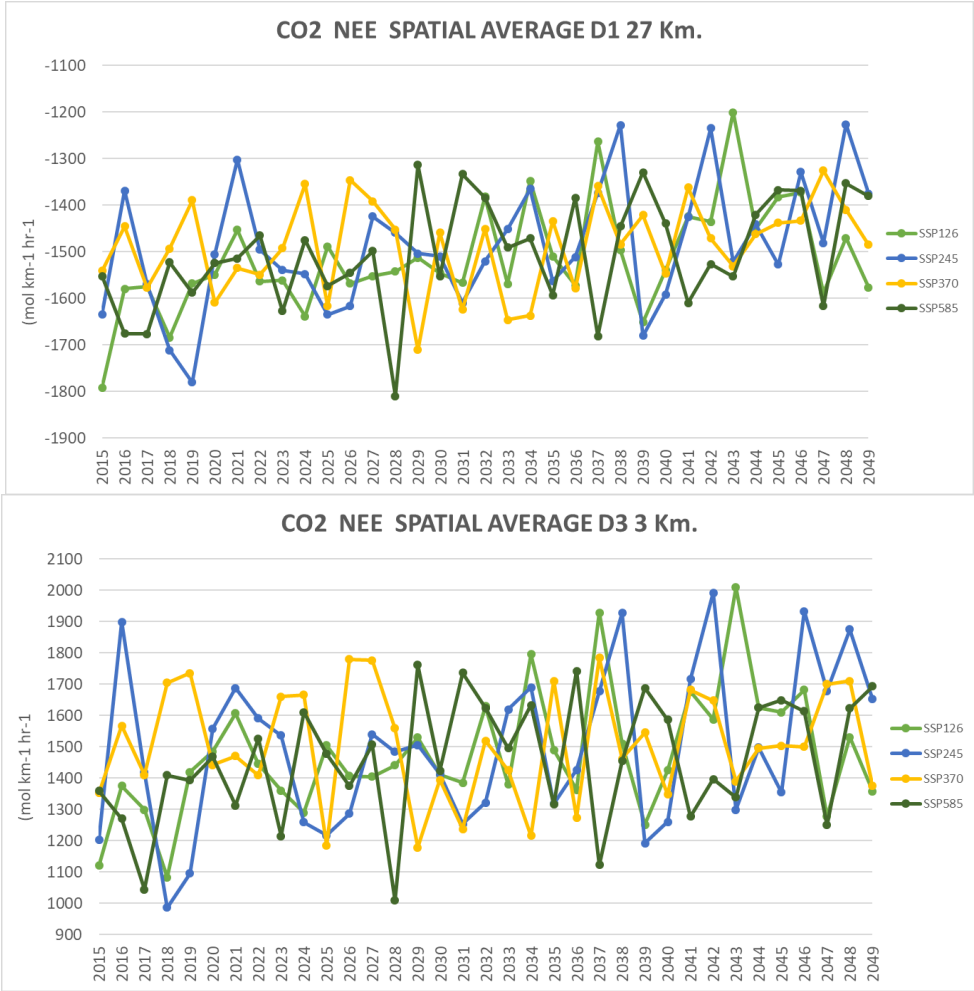

Figure 4. Temporal evolution of Net Ecosystem Exchange (NEE, CO_2 vegetation flux) [mol km^{-1} hr^{-1}]. Annual and spatially averaged values over the simulation domain of 27 km domain (D1) and 3km domain (D3) for each scenario, 2015–2049.

The figure 4 also reveals spatial differences in the behaviour of biogenic CO_2 fluxes between domains. Specifically, we observe that in Domain 1 (D1), which covers the entire Iberian Peninsula, net CO_2 removals dominate over emissions, indicating that, on average, vegetation in this wider region acts as a carbon sink. In contrast, in Domain 3 (D3) - which covers the Madrid metropolitan area - biogenic CO_2 emissions outweigh removals. This contrast can be attributed to a combination of vegetation type (in the north of the Peninsula there is much denser vegetation with higher absorption capacity than in the centre of the Peninsula), land cover heterogeneity and climatic conditions. In Domain 1, the presence of extensive forested and semi-natural areas with dense vegetation contributes to higher levels of gross primary productivity (GPP), thereby increasing net CO_2 uptake. In addition, these areas often experience more favourable microclimatic conditions (e.g. cooler temperatures and higher soil moisture) for photosynthesis, especially in elevated or coastal regions.On the other hand, Domain 3 includes urban and peri-urban landscapes, where vegetation is more fragmented and often consists of grasses, shrubs or ornamental species with lower photosynthetic efficiency. In addition, urban heat island effects and elevated temperatures can increase ecosystem respiration (RES), especially during summer months, thereby counteracting photosynthetic CO_2 uptake and resulting in net positive biogenic emissions.

When analyzing temporal trends across different climate scenarios, the simulations reveal a progressive decline in net CO_2 uptakes in Domain 1 (Iberian Peninsula) over time. While this domain maintains its role as a net carbon sink throughout the simulation period, the magnitude of uptake decreases slightly over time. This reduction is likely associated with climatic stress on vegetation, including higher temperatures. In Domain 3 (Community of Madrid), the results show an increase in net biogenic CO_2 emissions over the same period. Overall, both domains show a deterioration in the biogenic carbon balance. While Domain 1

experiences a reduction in its CO_2 sequestration capacity, Domain 3 transforms into a net biogenic CO_2 source. These trends highlight the sensitivity of biosphere CO_2 fluxes to climate change and suggest that even natural or semi-natural ecosystems could experience a weakening of their carbon sink function under future climate conditions.

4. CONCLUSIONS

In this study, we employed a high-resolution dynamic downscaling system (WRF/Chem-VPRM-EMIMO) to assess the impact of future climate scenarios on biogenic CO_2 fluxes in the Community of Madrid and the Iberian Peninsula as a whole. The modeling framework employed a nested approach with three spatial domains (27 km, 9 km, and 3 km resolution) and focused on the period 2015–2050. Four CMIP6 scenarios (SSP1-2.6, SSP2-4.5, SSP3-7.0, and SSP5-8.5) were upscaled from the global climate model MPI-ESM1.2-HR. To isolate climate effects, anthropogenic emissions, land use, and satellite vegetation indices were fixed at 2018 levels. Model performance was evaluated against hourly temperature observations from three meteorological stations in the Community of Madrid over the period 2015–2023. The WRF/Chem-VPRM model showed good agreement with observed data, with R^2 values above 0.80 in all scenarios. Among the scenarios, SSP5-8.5 presented the best overall fit to observations, although no substantial differences were found between scenarios in terms of model accuracy. All scenarios projected a gradual increase in average temperatures over the simulation period, with the largest increase in SSP3-7.0, exceeding SSP5-8.5 by approximately 0.22%.

Spatial analysis of the net CO_2 budget—combining biogenic and anthropogenic fluxes—revealed contrasting patterns across domains. The northern Iberian Peninsula and parts of the Community of Madrid function as carbon sinks, primarily due to their extensive vegetation cover. However, in the central metropolitan area of Madrid, anthropogenic and biogenic emissions predominate, resulting in a net source of CO_2. Despite these local emissions, Domain 1 (27 km resolution) still shows an overall net uptake of up to 1400 mol km^{-1} h^{-1}, with urban areas such as Madrid contributing positive local fluxes of up to 4500 mol km^{-1} h^{-1}. When analyzing the Net Ecosystem Exchange (NEE), we observed that the SSP3-7.0 scenario presented the largest increase in biogenic CO_2 emissions. This trend is attributed to rising temperatures, which enhance plant respiration more than photosynthesis, especially in semi-arid urbanized environments. The other scenarios also showed increases in emissions, albeit to a lesser extent, consistent with their more moderate temperature trends.

In the Community of Madrid, vegetation-related CO_2 emissions exceed absorptions in most areas, with the exception of mountainous areas, which remain net absorbers due to denser and more productive vegetation. This spatial heterogeneity underscores the importance of high-resolution modeling in urban and peri-urban landscapes. Regarding atmospheric CO_2 concentrations, the SSP3-7.0 scenario also showed a slight increase (~0.11%) relative to SSP5-8.5. On the other hand, the SSP1-2.6 and SSP2-4.5 scenarios projected small decreases in CO_2 concentrations. However, these variations are moderate, likely due to the strong influence of boundary conditions on CO_2 concentration fields.

As general conclusions of the study, we can highlight that climate change will reduce the capacity of ecosystems as carbon sinks due to increased respiration and thermal stress, while in urban areas, they will act as net sources of biogenic CO_2. High-resolution integrated modeling frameworks, such as WRF/Chem-VPRM-EMIMO, are essential for capturing spatial heterogeneity and generating valuable information for the development of mitigation and air quality strategies. Although the study was applied to the Community of Madrid, this modeling methodology is transferable to other regions and can help decision-makers assess the impact of local interventions—such as increased vegetation or agroforestry practices—on atmospheric CO_2 dynamics.

REFERENCES

Ahmadov, R., Gerbig, C., Kretschmer, R., Körner, S., Rödenbeck, C., Bousquet, P., and Ramonet, M.: Comparing high resolution WRF-VPRM simulations and two global CO2 transport models with coastal tower measurements of CO2, Biogeosciences, 6, 807–817, https://doi.org/10.5194/bg-6-807-510 2009, 2009.

Ballav S, Patra PK, Takigawa M, Ghosh S, De UK, Maksyutov S, Murayama S, Mukai H, Hashimoto S (2012) Simulation of CO2 concentration over East Asia using the regional transport model WRF-CO2. J Meteorol Soc Japan Ser II 90(6):959–976

Bezyk Y, Sówka I and Górka M 2021 Assessment of urban CO2 budget: anthropogenic and biogenic inputs Urban Clim. 39 100949

Davis K J et al 2017 The Indianapolis Flux Experiment (INFLUX): a test-bed for developing urban greenhouse gas emission measurements Elementa 5 21

Dong X, Yue M, Jiang Y, Hu X-M, Ma Q, Pu J, Zhou G (2021) Analysis of CO2 spatio-temporal variations in China using a weather–biosphere online coupled model. Atmos Chem Phys 21:7217–7233. https://doi.org/10.5194/acp-21-7217-2021

Eyring et al. 2016. Overview of the coupled model intercomparison project phase 6 (CMIP6) experimental design and organization. Geoscientific Model Development 9, 5 (May 2016), 1937–1958. DOI:http://dx.doi.org/10.5194/gmd-9-1937-2016

Grell GA, Dévényi D (2002) A generalized approach to parameterizing convection combining ensemble and data assimilation techniques. Geophys Res Lett 29:1693. https://doi.org/10.1029/2002GL015311

Hardiman B S, Wang J A, Hutyra L R, Gately C K, Getson J M and Friedl M A 2017 Accounting for urban biogenic fluxes in regional carbon budgets Sci. Total Environ. 592 366–72 Menzer and McFadden, 2017;

Hausfather Z, Peters GP. RCP8.5 is a problematic scenario for near-term emissions. Proc Natl Acad Sci U S A. 2020 Nov 10;117(45):27791-27792. doi: 10.1073/pnas.2017124117. Epub 2020 Oct 20. PMID: 33082220; PMCID: PMC7668049.

Hong S-Y, Noh Y, Dudhia J (2006) A new vertical diffusion package with an explicit treatment of entrainment processes. Mon Weather Rev 134:2318–2341

Hutyra L R, Duren R, Gurney K R, Grimm N, Kort E A, Larson E and Shrestha G 2014 Urbanization and the carbon cycle: current capabilities and research outlook from the natural sciences perspective Earths Future 2 473–95

Iacono MJ, Delamere JS, Mlawer EJ, Shephard MW, Clough SA, Collins WD (2008) Radiative forcing by long-lived greenhouse gases: calculations with the AER radiative transfer models. J Geophys Res: Atmos 113:D13103

IPCC 2014 Climate change 2014: synthesis report Contribution of Working Groups I, II and III to the Fifth Assessment Report of the Intergovernmental Panel on Climate Change (Geneva: IPCC) p 151.

Keywan Riahi, Detlef P. van Vuuren, Elmar Kriegler, Jae Edmonds, Brian C. Oâ€™Neill, Shinichiro Fujimori, Nico Bauer, Katherine Calvin, Rob Dellink, Oliver Fricko, Wolfgang Lutz, Alexander Popp, Jesus Crespo Cuaresma, Samir KC, Marian Leimbach, Leiwen Jiang, Tom Kram, Shilpa Rao, Johannes Emmerling, Kristie Ebi, Tomoko Hasegawa, Petr Havlik, Florian HumpenÃ¶der, Lara Aleluia Da Silva, Steve Smith, Elke Stehfest, Valentina Bosetti, Jiyong Eom, David Gernaat, Toshihiko Masui, Joeri Rogelj, Jessica Strefler, Laurent Drouet, Volker Krey, Gunnar Luderer, Mathijs Harmsen, Kiyoshi Takahashi, Lavinia Baumstark, Jonathan C. Doelman, Mikiko Kainuma, Zbigniew Klimont, Giacomo Marangoni, Hermann Lotze-Campen, Michael Obersteiner, Andrzej Tabeau, Massimo Tavoni,The Shared Socioeconomic Pathways and their energy, land use, and greenhouse gas emissions implications: An overview, Global Environmental Change, Volume 42, 2017, Pages 153-168, ISSN 0959-3780, https://doi.org/10.1016/j.gloenvcha.2016.05.009.

Mahadevan et al. 2008. A satellite-based biosphere parameterization for Net Ecosystem Co2 Exchange: Vegetation photosynthesis and respiration model (VPRM). Global Biogeochemical Cycles 22, 2 (April 2008). DOI:http://dx.doi.org/10.1029/2006gb002735

Meinshausen et al. (2020): The shared socio-economic pathway (SSP) greenhouse gas concentrations and their extensions to 2500. Geoscientific Model Development 13: 3571–3605. https://doi.org/10.5194/gmd-13-3571-2020.

Miller J B, Lehman S J, Verhulst K R, Miller C E, Duren R M, Yadav V, Newman S and Sloop C D 2020 Large and seasonally varying biospheric CO2 fluxes in the Los Angeles megacity revealed by atmospheric radiocarbon Proc. Natl Acad. Sci. 117 26681–7

Monin, A. S. and Obukhov, A. M.: Basic Laws of Turbulent Mixing in the Surface Layer of the Atmosphere, Tr. Akad. Nauk SSSR Geophiz. Inst., 24, 163–187, 1954.

Morrison, H., Thompson, G., and Tatarskii, V.: Impact of Cloud Microphysics on the Development of Trailing Stratiform Precipitation in a Simulated Squall Line: Comparison of One- and Two-Moment Schemes, Mon. Weather Rev., 137, 991–1007, https://doi.org/10.1175/2008MWR2556.1, 2009.

O'Neill et al. 2016. The scenario model intercomparison project (scenariomip) for CMIP6. Geoscientific Model Development 9, 9 (September 2016), 3461–3482. DOI:http://dx.doi.org/10.5194/gmd-9-3461-2016

Park C, Park S-Y, Gurney K R, Gerbig C, DiGangi J P, Choi Y and Lee H W 2020 Numerical simulation of atmospheric CO2 concentration and flux over the Korean Peninsula using WRF VPRM model during Korus-AQ 2016 campaign PLoS One 15 e0228106

Pillai D, Gerbig C, Ahmadov R, Rödenbeck C, Kretschmer R, Koch T, Thompson R, Neininger B, Lavrié JV (2011) High-resolution simulations of atmospheric CO2 over complex terrain - representing the Ochsenkopf mountain tall tower. Atmos Chem Phys 11:7445–7464

Powers JG, Klemp JB, Skamarock WC, Davis CA, Dudhia J, Gill DO, Coen JL, Gochis DJ, Ahmadov R, Peckham SE, Grell GA, Michalakes J, Trahan S, Benjamin SG, Alexander CR, Dimego GJ, Wang W, Schwartz CS, Romine GS, Liu Z, Snyder C, Chen F, Barlage MJ, Yu W, Duda MG (2017) The weather research and forecasting model: overview, system efforts, and future directions. Bull Am Meteor Soc 98(8):1717–1737

San José et al. 2015. Sensitivity of feedback effects in CBMZ/Mosaic Chemical Mechanism. Atmospheric Environment 115 (August 2015), 646–656. DOI:http://dx.doi.org/10.1016/j.atmosenv.2015.04.030

S. Hu, T. Zhou Skillful prediction of summer rainfall in the Tibetan Plateau on multiyear time scales Sci. Adv., 7 (24) (2021), Article eabf9395, 10.1126/sciadv.abf9395

Sówka I and Bezyk Y 2018 Greenhouse gas emission accounting at urban level: a case study of the city of Wroclaw (Poland) Atmos. Pollut. Res. 9 289–98

T. Cui, C. Li, F. Tian Evaluation of temperature and precipitation simulations in CMIP6 models over the Tibetan plateau

Tewari M, Chen F, Wang W, Dudhia J, LeMone MA, Mitchell K, Ek M, Gayno G, Wegiel J, Cuenca RH (2004) Implementation and verification of the unified NOAH land surface model in the WRF model. 20th conference on weather analysis and forecasting/16th conference on numerical weather prediction (Vol. 1115). Seattle, WA: American Meteorological Society

Y.-Y. Zhu, S. Yang Evaluation of CMIP6 for historical temperature and precipitation over the Tibetan Plateau and its comparison with CMIP5 Adv. Clim. Change Res., 11 (3) (2020), pp. 239-251, 10.1016/j.accre.2020.08.001

W. A. Müller, J. H. Jungclaus, T. Mauritsen, J. Baehr, M. Bittner, R. Budich, F. Bunzel, M. Esch, R. Ghosh, H. Haak, T. Ilyina, T. Kleine, L. Kornblueh, H. Li, K. Modali, D. Notz, H. Pohlmann A Higher-resolution Version of the Max Planck Institute Earth System Model (MPI-ESM1.2-HR) First published: 31 May 2018 https://doi.org/10.1029/2017MS001217

Declarations

Ethics approval and consent to participate

All authors have followed the ethics rules and have approved to participate.

Consent for publication

All authors have provided the consent to publish this research paper.

Availability of data and material

The datasets generated during and/or analysed during the current study are available in the project website: https://distender.eu/

Competing Interests

The authors have no relevant financial or non-financial interests to disclose

Funding

This work was supported by European Union's Horizon EU research, grant agreement No 101056836

Authors Contributions

All authors have contributed significantly to this work in their respective areas of expertise, ensuring a comprehensive and multidisciplinary approach to the subject. RSJ prepared the initial draft, outlining the main concepts, methodologies and conclusions. This draft was revised, expanded and refined by JLP and MG, who contributed critical ideas, additional data and methodological improvements based on their specific experience. All authors carefully reviewed the final version of the manuscript, gave their approval, and agreed to its submission.